AccR is a master regulator involved in carbon catabolite repression of the anaerobic catabolism of aromatic compounds in *Azoarcus* sp. CIB*

J. Andrés Valderrama[‡1], Victoria Shingler[§], Manuel Carmona[‡] , and Eduardo Díaz[‡2]

From the [‡]Department of Environmental Biology, Centro de Investigaciones Biológicas-Consejo Superior de Investigaciones Científicas, 28040 Madrid, Spain and the [§]Department of Molecular Biology, University of Umeå, 90187 Umeå, Sweden

[1] Recipient of a FPI fellowship from the Ministry of Economy and Competitiveness of Spain.

[2] To whom correspondence should be addressed: Dept. of Environmental Biology, Centro de Investigaciones Biológicas-Consejo Superior de Investigaciones Científicas, Ramiro de Maeztu 9, 28040 Madrid, Spain. Tel.: 34-918373112; Fax: 34-915360432; E-mail: ediaz@cib.csic.es

* This work was supported by the Ministry of Economy and Competitiveness of Spain (BIO2009-10438, CSD2007-00005, BIO2012-39501), EU FP7 Grant 311815, and The Swedish Research Council (Grant 621-2011-4791).

Running title: *The AccR response regulator from Azoarcus sp. CIB*

Keywords: carbon catabolite repression, transcriptional regulation, response regulator, *Azoarcus*, anaerobic degradation

[3]The abbreviations used are: CCR, carbon catabolite repression; HTH motif, helix-turn-helix motif; REC motif, receiver motif.

CAPSULE

Background: Mechanisms underlying carbon catabolite repression (CCR) control of the anaerobic degradation of aromatic compounds have previously remained elusive.
Results: Phosphorylated AccR was identified as a transcriptional repressor of aromatics degradation operons expressed under anaerobic conditions.
Conclusion: The response regulator AccR controls the succinate-dependent CCR in *Azoarcus* sp. CIB.
Significance: AccR is a master regulator that controls anaerobic CCR in bacteria.

ABSTRACT

Here we characterized the first known transcriptional regulator that accounts for carbon catabolite repression (CCR) control of the anaerobic catabolism of aromatic compounds in bacteria. The AccR response regulator of *Azoarcus* sp. CIB controls succinate-responsive CCR of the central pathways for the anaerobic catabolism of aromatics by this strain. Phosphorylation of AccR to AccR-P triggers a monomer-to-dimer transition, as well as the ability to bind to the target promoter and cause repression both in vivo and in vitro. Substitution of the Asp^{60} phosphorylation residue of the N-terminal receiver motif of AccR, to a phosphor-mimic Glu residue, generates a constitutively active derivative that behaves as a super-repressor of the target genes. AccR-P binds in vitro to a conserved inverted repeat (ATGCA-N_6-TGCAT) present at two different locations within the P_N promoter of the *bzd* genes for anaerobic benzoate degradation. Because the DNA-binding proficient C-terminal domain of AccR is monomeric, we propose an activation mechanism in which phosphorylation of Asp^{60} of AccR alleviates inter-domain repression mediated by the N-terminal domain. The presence of AccR-like proteins encoded in the genomes of other β-proteobacteria of the *Azoarcus/Thauera* group further suggests that AccR constitutes a master regulator that controls anaerobic CCR in these bacteria.

Carbon catabolite repression (CCR)[3] is wide spread in bacteria and imparts a competitive advantage and improved fitness by establishing priorities in carbon utilization. This enables bacteria to optimizing growth rates in natural environments that provide complex mixtures of nutrients. Regulatory mechanism of CCR operate through subverting expression of genes required for the uptake and/or metabolism of secondary (less preferred) carbon sources in the presence of a preferred substrate (1). Such secondary carbon sources include aromatic compounds which, after carbohydrates, are the most widely distributed class of organic compounds in nature.

Where studied, CCR mechanisms impact expression of pathways for the degradation of aromatic compounds. In contrast to enterics such as *Escherichia coli*, which utilize glucose as the preferred carbon source, soil bacteria e.g. *Pseudomonas* metabolize many organic acids or amino acids in preference to sugars (2). However, not all organic acids mediate CCR, nor do all organic acids provoke the same effect in different microorganisms (3,4).

The regulatory elements involved in CCR of aerobic catabolism of aromatic compounds in different bacteria are diverse (2,4-8). In *E. coli* the cAMP-responsive CRP transcriptional regulator imparts CCR control over catabolism of aromatic compounds (8). In *Pseudomonas* strains, the Crc protein exerts CCR on the assimilation of certain aromatic compounds (9-11) as well as some sugars and amino acids (12-14). In contrast to CRP, Crc acts post-transcriptionally (3,4,15). Other proteins described to be involved in CCR control of aerobic catabolism of aromatics in *Pseudomonas* include PtsN and PtsO (nitrogen phosphotransferase system) (6,16) and the redox-responsive *o*-type terminal oxidase CyoB (17,18), while in *Acidovorax* sp. KKS102, CCR of biphenyl degradation in response to some organic acids is mediated by the response regulator BphQ (7).

Far less is known about CCR control of anaerobic catabolism of aromatic compounds, although cases of this phenomenon have been reported. For

example, some organic acids cause CCR of genes involved in the anaerobic degradation of aromatic compounds in *Thauera aromatica* (19) and *Azoarcus* sp. CIB (20), while in closely related strains such as *Aromatoleum aromaticum* EbN1, aromatic compounds are preferred carbon source over aliphatic organic acids (21). However, the mechanism(s) underlying CCR in these cases are still unknown.

Elucidating the molecular mechanism(s) underlying CCR is important for both basis understanding of how metabolism is regulated in the environment and for potential biotechnological applications such as optimizing bioremediation strategies and the design of tailor-made biocatalysts/biosensors (4). This is particullaly relevant for aromatic compounds that are difficult to degrade and tend to accumulate in the environment under both aerobic and anaerobic conditions. In this work we sought to use the denitrifying β-proteobacterium *Azoarcus* sp. CIB to analyse the mechanism(s) underlying CCR of anaerobic pathways for the dissimilation of aromatic compounds. *Azoarcus* sp. CIB is able to degrade aromatic compounds both aerobically and anaerobically (20,22) and it has been used as a model organism to study the specific regulation of the benzoyl-CoA central pathways for the aerobic (*box* genes) and anaerobic (*bzd* genes) degradation of benzoate (20, 23-27).

The *Azoarcus* sp. CIB *bzd* genes responsible for the anaerobic degradation of benzoate are clustered and consist of the P_N promoter driven *bzdNOPQMSTUVWXYZA* catabolic operon and the *bzdR* regulatory gene (20). BzdR-mediated repression of P_N is alleviated by the inducer molecule benzoyl-CoA, the first intermediate of the catabolic pathway (23,24). However, activity of the P_N promoter also strictly requires the AcpR transcriptional activator – an orthologue of the *E. coli* Fnr global regulator – which specifically drives expression of the *bzd* catabolic operon in an oxygen-dependent manner (25). In addition to this dual repressor / activator control, the P_N promoter is also subject to control by the benzoyl-CoA dependent BoxR repressor – a BzdR paralog that regulates the expression of the *box* genes – indicating the existence of cross-regulation between the aerobic and anaerobic benzoate degradation pathways of *Azoarcus* sp. CIB (27).

In our previous work we found that anaerobic expression of the *bzd* genes from the P_N promoter is additionally subject to CCR control in response to organic acids such as succinate, malate and acetate (20), although the mechanism(s) underlying this level of control was not determined. In this work we report the characterization of AccR as a response regulator that mediates anaerobic CCR control on the P_N promoter. Based on our finding that AccR exerts anaerobic CCR control on central pathways for catabolism of other aromatics in *Azoarcus* sp. CIB, AccR constitutes the first master regulator described that controls CCR of anaerobic catabolism of aromatic compounds in bacteria. Because of the existence of AccR orthologs within the genomes of closely related *Azoarcus*/*Thauera* strains, we suggest that AccR is likely the global mediator of CCR control for anaerobic assimilation of aromatic compounds in this group of β-proteobacteria.

EXPERIMENTAL PROCEDURES

Bacterial Strains, Plasmids and Growth Conditions-Bacterial strains and plasmids used are listed in Table 1. Plasmids were constructed by standard molecular techniques (35) with the fidelity of all PCR-derived DNA (Table 2) verified by sequencing. *E. coli* cells were routinely grown at 37ºC in Lysogeny broth (LB) medium (35). When required, *E. coli* $AFMCP_N$ was grown aerobically or anaerobically (using 10 mM nitrate as terminal electron acceptor) at 30ºC in M63 minimal medium (36), supplemented with 0.1 mg/ml thiamine and 20 mM glycerol as the carbon source. *Azoarcus* strains were similarly grown aerobically or anaerobically at 30ºC in MC medium containing the indicated carbon source(s) as described previously (20). Where appropriate, antibiotics were added at the following concentrations: ampicillin (Ap, 100 μg/ml), kanamycin (Km, 50 μg/ml), gentamicin (Gm, 7.5 μg/ml), and streptomycin (Sm, 50 μg/ml). An AccR null derivative of *Azoarcus* sp. CIB was generated by homologous recombination

using the R6K-based suicide plasmid pKNG101ΔaccR (Table 1) that allows positive selections of double site recombinants using the *sacB* gene of *Bacillus subtilis* (31). Conjugation of pKNG101ΔaccR from replication-permissive *E. coli* SM10 λ*pir* was used to introduce the plasmid into *Azoarcus* sp. CIB. Derivatives containing first site recombinants were selected on streptomycin-containing MC medium with 10 mM glutarate as the sole carbon source. Second site recombination was selected by growth on the same medium supplemented with 5% sucrose. Correct allelic exchange in sucrose resistant and streptomycin sensitive derivatives was verified using primers 5´AccRmut (BamHI) and 3'AccRmut(SpeI) (Table 2).

Sequence Analyses and Molecular Modelling-The nucleotide sequence of the *accR* gene of *Azoarcus* sp. CIB has been submitted to the GenBank with accession number KF233996. Pairwise and multiple sequence alignments of AccR-like proteins were made with the CLUSTALW (37) program at the EMBL-EBI server (http://www.ebi.ac.uk/Tools/msa/clustalw2/). Phylogenetic analysis, carried out according to Kimura´s two-parameter method (38), was reconstructed using the neighbour-joining method (39) PHYLIP program (40).

β-Galactosidase Assays-The β-galactosidase activities from promoter-*lacZ* reporter fusions were measured with permeabilized cells, when cultures reached mid-exponential phase, as described by Miller (36).

Purification of AccR Derivatives-His-tagged AccR derivatives, all with a 13 amino acid (MRGSHHHHHHGIL) N-terminal fusion, were expressed from the isopropyl-1-thio-ß-D-galactopyranoside (IPTG) inducible T5 promoter of pQE32 expression vector (His_6AccR from pQE32-His_6AccR, His_6AccRD60E from pQE32-His_6AccRD60E, and His_6CAccR from pQE32-His_6CAccR; Table 1). Proteins were purified from *E. coli* M15 that additionally harboured pREP4, a LacI expression plasmid that aids IPTG-dependent expression. Cultures were grown at 37°C until the mid-exponential growth phase in LB containing appropriate antibiotics and then expression was induced by the addition of IPTG (0.1 mM). After a further 5 hours incubation, cells were harvested from 1 litre of culture at 4°C, resuspended in 25 ml lysis buffer [50 mM NaH_2PO_4, pH 8.0, 300 mM KCl, 20 mM imidazol] and disrupted by passage through a French press (Aminco Corp.) operated at a pressure of 20,000 p.s.i. Cell lysates were clarified by centrifugation (26,000 x *g* for 25 min at 4°C) prior to loading on nickel-nitrilotriacetic acid-agarose columns (Qiagen) equilibrated with lysis buffer. Columns were washed at 4°C with 50 volumes of lysis buffer and the His-tagged proteins subsequently eluted with elution buffer [50 mM NaH_2PO_4, pH 8.0, 300 mM KCl, 75 mM imidazol]. Peak fractions were pooled, dialyzed at 4°C into modified FP buffer [20 mM Tris-HCl, pH 7.5, 5% glycerol, and 50 mM KCl], and stored as independent aliquots at -20 °C.

In vitro Phosphorylation of AccR Derivatives-AccR and its derivatives were phosphorylated by treatment with 20 mM carbamoyl phosphate in phosphorylation buffer [20 mM Pipes, 10 mM magnesium acetate, 10 mM KCl, 170 mM NaCl, and 5% (vol/vol) glycerol, pH 7.5] for 90 min at 28°C.

Mass Spectrometry Analyses-Mass spectrometry experiments with the AccR and AccR-P proteins (20 μM) were performed on an Autoflex III MALDI-TOF-TOF instrument (Bruker Daltonics, Bremen, Germany) with a smartbeam laser. Spectra were acquired using a laser power just above the ionization threshold. Samples were analysed in the positive ion detection and delayed extraction linear mode. Typically, 1000 laser shots were summed into a single mass spectrum. External calibration was performed using bovine albumin (Sigma), covering the range from 30.000 to 70.000 Da. A saturated solution of sinapinic acid in 3:1 water/acetonitrile and 0.1% trifluoroacetic acid was used as the matrix. For sample preparation, the sample solution and the matrix were premixed (1:1, v/v) and then 1 μl of the mixture was spotted on the stainless steel

target and allowed to dry at room temperature.

Analytical Ultracentrifugation Methods-Analyses were performed using several protein concentrations (from 5 to 40 μM) equilibrated with 20 mM Tris HCl pH 7.5 / 50 mM KCl / 5% glycerol buffer. Sedimentation velocity runs (48,000 rpm at 20°C) were carried out in an XL-I analytical ultracentrifuge (Beckman-Coulter Inc.) equipped with UV-Visible optic detection system, using an An50Ti rotor and 12 mm double sector centrepiece. Sedimentation profiles were registered every 1–5 min at 280 nm in the experiments with His_6-AccR and His_6-AccR-P, and 235 nm in the experiments with His_6-CAccR. Sedimentation coefficient distributions were calculated by least squares boundary modelling of sedimentation velocity data using the *c*(*s*) method (41), as implemented in the SEDFIT program. These *s* values were corrected to standard conditions (water at 20°C, and infinite dilution) using the SEDNTERP program (42) to obtain the corresponding standard *s* values ($s_{20,w}$). Sedimentation equilibrium assays were carried out using the same experimental conditions and instrument as in the sedimentation velocity experiments, with speeds ranging from 5,000 to 15,000 rpm (depending upon the sample analyzed) and at several wavelengths (235, 260, 280, and 290 nm) with short columns (85–95 μl). After each equilibrium scan, a high speed centrifugation run (40,000 rpm) was performed to estimate the corresponding base-line offset. The measured low speed equilibrium concentration (signal) gradients of His_6-AccR, His_6-AccR-P and His_6-CAccR were fitted using an equation that characterizes the equilibrium gradient of an ideally sedimenting solute (using a MATLAB program, kindly provided by Dr. Allen Minton, National Institutes of Health) to obtain the corresponding buoyant signal average molecular weight.

Gel Retardation Assays-Gel retardation reaction mixtures (9 μl) contained FP buffer [20 mM Tris-HCl, pH 7.5, 10% glycerol, 2 mM β-mercaptoethanol, 50 mM KCl], 0.05 nM ^{32}P-labelled DNA probe, 250 μg/ml bovine serum albumin, 50 μg/ml herring sperm (competitor) DNA, and the indicated concentration of purified protein. After incubation for 20 min at 30ºC, samples were analyzed by electrophoresis using 5% polyacrylamide gels buffered with 0.5 x TBE (45 mM Tris-borate, 1 mM EDTA). Dried gels were subsequently imaged using Hyperfilm MP (Amersham Biosciences). Radiolabelled DNA probes [P_N (376 bp), P_{N2} (162 bp), P_{N3} (93 bp) P_{N2mut} (165 bp), P_{B1} (251 bp), and P_D (234 bp)] were generated by PCR amplification (Table 2). For all but the P_{B1} probe, ^{32}P was incorporated by the use of a primer 5'-end labelled with phage T4 polynucleotide kinase and [γ-^{32}P]ATP (3000 Ci/momol, Perkin-Elmer Life Sciences). For the P_{B1} probe, ^{32}P was incorporated by digestion of the PCR derived DNA with EcoRI and subsequent filling in of the resulting overhang end with [α-^{32}P]dATP (6000 Ci/mmol; Perkin Elmer) and the Klenow fragment of *E. coli* DNA polymerase I.

DNaseI Footprinting Assays-DNaseI footprinting reactions (15 μl) in FP buffer contained 2 nM radiolabelled P_N probe (see above), 1 mg/ml bovine serum albumin, and the indicated concentration of *in vitro* phosphorylated His_6-AccR (AccR-P). Reactions were incubated for 20 min at 25ºC, prior to addition of 3 μl (0.05 units) of DNase I solution [prepared in 10 mM $CaCl_2$, 10 mM $MgCl_2$, 125 mM KCl, and 10 mM Tris-HCl, pH 7.5]. After 20 s incubation at 37°C, reactions were quenched by the addition of 180 μl of a solution containing 0.4 M sodium acetate, 2.5 mM EDTA, 50 μg/ml calf thymus DNA, and 0.3 μg/ml glycogen. DNA fragments were phenol extracted, precipitated and analysed as previously described (23). An A+G reaction (43) was carried out with the same fragment. Images were obtained as described for gel retardation assays.

In vitro Transcription Experiments-Multiple-round *in vitro* transcription reactions (50 μl) were performed essentially as previously described (25) in a buffer consisting of 40 mM Tris-HCl pH 7.5, 100 mM KCl, 10 mM $MgCl_2$, 0.1 mM bovine serum albumin and 10 mM dithiothreitol.

Reactions contained 5 nM of supercoiled plasmid pJCD-P_N as the DNA template, 50 nM *E. coli* σ^{70}-RNA polymerase (1U/µl; USB), 200 nM His_6-Fnr* activator (a constitutively active Fnr derivative that is able to promote transcription in the presence of oxygen) (25,44) and different concentrations of purified AccR or AccR-P proteins. Reactions were equilibrated for 10 min at 37ºC prior to initiation of transcription by the addition of nucleotides [final concentrations: 500 nM of ATP, CTP, and GTP; 50 nM UTP; and 1µCi of [α-^{32}P]UTP (3,000 mCi/mmol; Perkin Elmer)]. After incubation for 20 min at 37°C, reactions were terminated by the addition of an equal volume of a solution containing 50 mM EDTA, 350 mM NaCl and 0.5 mg/ml of carrier tRNA. Ethanol precipitated transcripts were dissolved in loading buffer (7 M urea, 1 mM EDTA, 0.6 M glycerol, 0.9 mM bromophenol blue, and 1.1 mM xylene cyanol), resolved by electrophoresed on a denaturing 7 M urea / 4% polyacrylamide gel, and visualized by autoradiography.

Real-time RT-PCR Assays-Total RNA was extracted and DNase I treated using reagents provided with the RNeasy Mini Kit (Qiagen) according to the manufacturer instructions. The concentration and purity of the RNA samples were assessed using an ND1000 spectrophotometer (Nanodrop Technologies) according to the manufacturer´s protocols. Synthesis of total cDNA was performed in 20 µl reactions containing 1 µg RNA, 0.5 mM of each dNTP, 200 U of SuperScript II reverse transcriptase (Invitrogen), and 5 µM of random hexamers in the buffer provided by the manufacturer. Samples were initially heated at 65ºC for 5 min and then incubated at 42°C for 2 h. Reactions were terminated by incubation at 70°C for 15 min and the cDNA further purified using Geneclean Turbo kit (MP Biomedicals). An IQ5 Multicolor Real-Time PCR Detection System (Bio-Rad) was used for real-time PCR of triplicate samples. Reactions (25 µl) containing 5 ng cDNA, 0.2 µM of two target specific primers, and 12.5 µl SYBR Green Mix (Applied Biosystems). Primer pairs used to amplify transcripts from the P_D and P_N promoters and the transcript of the *dnaE* gene (encoding the α-subunit of DNA polymerase III) as an internal control to normalize the sample data are given in Table 2. Amplifications were carried with 1 denaturation cycle (95°C for 4 min), followed by 30 cycles of amplification (95°C for 1 min; 60°C for 1 min; 72°C for 30 s). After amplification, melting curves were generated to confirm amplification of a single product. For relative quantification, a calibration curve was constructed for each amplicon by using five-fold serial dilutions of *Azoarcus* sp. CIB genomic DNA ranging from 2.5 ng to 1.6 x10^{-6} ng. These standard curves were used to extrapolate the relative abundance of the cDNA targets within the linear range of the curve. Results were normalized relative to those obtained for the *dnaE* internal control.

RESULTS

The accR Gene Is Required for CCR Control of the bzd Genes in Azoarcus sp. CIB-In silico analysis of the unpublished draft *Azoarcus* sp. CIB genome sequence identified a gene – hereafter referred to as *accR* (aromatic catabolic control regulator; accession number KF233996) – whose product shows 47% amino acid sequence identity with the response regulator BphQ involved in CCR control of the biphenyl degradation pathway in *Acidovorax* sp. KKS102 (7). Orthologs of *accR* are also found in the genomes of other *β*-proteobacteria *Azoarcus* and *Thauera* strains (Supplemental Fig. S1). These observations prompted us to test AccR as a potential candidate for CCR control of the assimilation of aromatic compounds in *Azoarcus* sp. CIB. To this end we generated an AccR null derivative (*Azoarcus* sp. CIBΔ*accR*, Table 1), and measured the activity of the P_N promoter, which drives the anaerobic expression of the *bzd* genes, in comparison to P_N activity in the wild type strain. Transcripts from P_N were monitored by real-time RT-PCR using RNA extracted from cultures grown anaerobically at the expense of benzoate alone (control condition) or benzoate plus succinate (CCR condition). As shown in Fig. 1, both strains exhibited similar levels

of P_N activity when grown on benzoate, but the AccR null mutant was unable to exert CCR control in response to succinate – a defect that could be complemented by introduction of plasmid pBBR5AccR (Table 1) carrying *accR* under control of the *Plac* promoter. Hence, these results support the idea that AccR acts to repress the P_N promoter under CCR conditions.

AccR Possess in vitro Properties of Response Regulators-Sequence comparisons indicated that AccR belongs to the FixJ/NarL family of response regulators (45-47). AccR exhibits the typical two-domain architecture of this class of proteins, consisting of an N-terminal domain (NAccR; residues 1-122) and a C-terminal region (CAccR; residues 145-212) connected by a 23-residues long linker (Supplemental Fig. S1*A*). The NAccR domain contains the highly conserved receiver (REC) motif (residues 20-122) (Supplemental Fig. S1*A*), that is involved in phosphorylation and dephosphorylation reactions of response regulators (48). The CAccR domain contains a NarL/FixJ helix-turn-helix (HTH) DNA-binding motif (residues 162-189) responsible for interaction with the DNA (Supplemental Fig. S1*A*).

To determine whether AccR behaves as a typical response regulator *in vitro*, we expressed and purified a N-terminally His-tagged version of the AccR protein (His_6-AccR). Response regulators usually receive a phosphate group from a cognate histidine kinase in intact cells; however, REC motifs can also catalyze autophosphorylation using small phosphodonor molecules such as carbamoyl phosphate or acetyl phosphate (48). Hence, we analysed purified AccR before and after treatment with carbamoyl phosphate. Mass spectrometry analysis of untreated AccR revealed a single peak that corresponds to the theoretical mass of monomeric AccR (24,629 Da; Fig. 2*A*). When carbamoyl phosphate treated AccR was similarly analysed, two peaks were resolved – one corresponding to the unadorned monomer and the other compatible with the addition of a phosphate group (24,708.6 Da; Fig. 2*B*). We conclude from these results that AccR becomes phosphorylated (AccR-P) in the presence carbamoyl phosphate.

Analysis of the REC motif suggested that autophosphorylation of the AccR protein would occur at the highly conserved Asp^{60} residue that is located at the C-terminal end of β3-strand (Supplemental Fig. S1*A*). To experimentally verify this supposition, we purified a His-tagged mutant variant with Asp^{60} substituted to Glu (AccRD60E), a substitution that serves as a phospho-mimic in some response regulators (49,50). In contrast to the wild-type protein, AccRD60E exhibited no change in mass upon treatment with carbamoyl phosphate, supporting the idea that Asp^{60} is the target residue for AccR autophosphorylation.

AccR Undergoes a Monomer-to-Dimer Shift upon Phosphorylation-Phosphorylation of some response regulators results in a change in their oligomeric state (51). To determine if such a change occurs with AccR, we performed analytical ultracentrifugation analyses with different concentrations (5 to 40 μM) of untreated and carbamoyl phosphate treated AccR. Sedimentation velocity analysis of 10 μM of untreated AccR revealed a single species with an *s* value of 1.5 S (Fig. 2*C*). Carbamoyl phosphate treatment resulted in two species of similar abundance, one with an *s* value of 1.5 S and another one with an *s* value of 2.1 S (Fig. 2*D*), suggesting that ~50% of AccR becomes phosphorylated under the experimental conditions used.

The molecular weight of the 1.5 S species, as measured by sedimentation equilibrium (24,000 +/- 500 Da), is compatible with the mass of the AccR monomer (Fig. 2*E*, squares). However, since the frictional ratio f/f_0 of untreated AccR was 1.7, the shape deviates from that expected for a globular protein and suggest an elongated monomer. Sedimentation equilibrium experiments of the carbamoyl phosphate-treated AccR sample indicated a molecular mass (38,500+/- 400 Da) between that of a monomer and a dimer of the protein (Fig. 2*E*, circles), which is in agreement with the co-existence of approximately equal amounts of the 1.5 S (monomer) and 2.1 S (dimer) species within this preparation (Fig. 2*D*). Together, these

results demonstrate that unmodified AccR exists primarily as an elongated monomer, while phosphorylation induces a monomer-to-dimer transition but does not significantly change the global shape of the protein that retains a frictional ratio f/f_0 of 1.7.

DNA Binding by AccR Is Phosphorylation Dependent-Having established that AccR undergoes a phosphorylation-dependent conformational change (Fig. 2) and influences expression of *bzd* genes through the P_N promoter (Fig. 1), we next determined the ability of AccR to bind to DNA. For this we used a 376-bp DNA fragment spanning from -293 to +83 with respect to the transcription start site of the P_N promoter (P_N probe) in gel-retardation assays. The AccR protein was unable to bind to the P_N probe unless phosphorylated by prior carbamoyl phosphate treatment (Fig. 3*A* and *B*), while the Asp^{60} to Glu phospho-mimic substitution in AccRD60E rendered the protein DNA-binding competent in its non-phosphorylated state (Fig. 3*C*). These results show that the DNA binding capacity of AccR is dependent on its phosphorylated state, which can be mimicked by an Asp^{60} to Glu substitution. Because phosphorylation induces a monomer-to-dimer transition, it appears likely that AccR binds DNA primarily as a dimer.

AccR Binds to Palindrome Operator Sites within P_N to Confer CCR Control-To further characterize the DNA binding sites of AccR-P within the P_N promoter we performed DNase I footprinting assays. As shown in Fig. 4*A*, AccR-P protected a DNA region spanning from position -34 to -153 with respect to the transcription start site of the P_N promoter. This protected region contains two repetitions of the palindromic sequence (ATGCA-N_6-TGCAT) – denoted OR1 (from -67 to -82) and OR2 (from -130 to -145), see Fig. 4*B*. To determine if AccR-P was able to recognize the two palindromic regions independently, we used two probes, P_{N2} that spans OR1 and P_{N3} that spans OR2 (Fig. 4*B*), in gel-retardation assays. AccR-P bound to both probes with an affinity similar to that observed with the complete P_N probe (compare Fig. 4*C* and *D*, with Fig. 3*B*), indicating that AccR-P is able to recognize and bind to two different operator regions within the P_N promoter. To verify the role of the ATGCA-N_6-TGCAT palindrome in AccR-binding to P_N, we constructed a mutant derivative of the P_{N2} probe (P_{N2mut}) in which the left-half site of OR1 (ATGCA) was replaced by the sequence CCCTG. As shown in Fig. 4*E*, AccR-P was unable to bind to the P_{N2mut} probe. Similarly, AccR-P was unable to bind a truncated P_{N2} probe lacking the left-half site of OR1 (data not shown).

The results above demonstrate that AccR-P independently binds to two palindromic operator regions within the P_N promoter. To confirm that the AccR operator regions are the ones responsible of the carbon catabolite control of P_N, we constructed a truncated P_N promoter that lacks the AccR binding regions ($P_{N1;}$ -61 to +79) in a P_{N1}::*lacZ* fusion reporter plasmid and compared its activity to that of an otherwise identical wild type P_N::*lacZ* reporter plasmid in *Azoarcus* sp. CIB. As anticipated, the P_{N1}::*lacZ* fusion was essential immune to CCR control in response to succinate (Fig. 4*F*).

AccR Acts as a Repressor of the P_N Promoter in vitro-Our *in vivo* experiments (Figs. 1 and 4*F*) suggested a repressor role for AccR on transcription from the P_N promoter, which is consistent with the location of the AccR-P binding region spanning -35 to -153 (Fig. 4). To confirm this hypothesis, we performed *in vitro* transcription assays using a supercoiled DNA template bearing the P_N promoter. Within these assays, activity from P_N was elicited by constant concentrations of RNA polymerase and the Fnr* activator – an *E. coli* homolog of the AcpR activator of P_N that retains activity in the presence of oxygen (25). The effect of different concentrations of AccR or AccR-P on P_N output was then assessed. Whereas the formation of the expected 184-nucleotides transcript due to the activity of the P_N promoter was unperturbed by the presence of AccR (Fig. 5, *lanes 5* to *7*), levels of this transcript decreased in the presence of increasing amounts of AccR-P (Fig. 5, *lanes 2* to *4*). These data confirm the

repressor role of AccR and demonstrate that its inhibitory action on P_N activity is strictly dependent on the phosphorylated status of AccR.

CAccR Functions as an Independent Monomeric DNA Binding Domain-As outlined in the preceding sections, Asp^{60} within the REC motif of the NAccR domain is involved in autophosphorylation and CAccR contains the NarL/FixJ helix-turn-helix (HTH) DNA-binding motif predicted to mediate DNA binding. To determine if CAccR could function independently in this capacity, we purified a His-tagged version of CAccR (His_6-CAccR) and monitored its DNA binding capacity in gel-retardation assays using the P_N probe (as in Fig. 3). The data in Fig. 6*A* demonstrate that CAccR binds to the P_N probe in a concentration-dependent manner, experimentally verifying that this domain functions as an independent DNA binding domain.

Because phosphorylation of AccR provokes a monomer-to-dimer transition, we also determined the oligomeric status of CAccR as previously described for full length AccR. Sedimentation velocity experiments revealed a single species of CAccR with an *s* value of 1.1 S (Fig. 6*B*). The molecular weight of the 1.1 S species, as measured by sedimentation equilibrium of CAccR at different concentrations, is compatible with the mass of a monomer (Fig. 6*C*). We conclude from this data that under our experimental conditions, DNA-binding proficient CAccR is a monomer in solution. As expanded upon in the discussion, this suggests that dimerization of AccR after phosphorylation is carried out through the N-terminal domain, and that dimerization is not a prerequisite for DNA binding *per se*.

AccRD60E Acts as a Super-repressor-The Asp^{60} to Glu substitution renders AccR constitutively active (i.e. phosphorylation independent) in terms of its DNA binding capacity (Fig. 3*C*). Therefore, we were interested to test if it also exhibited constitutive repressor activity *in vivo*. To this end we used the heterologous *E. coli* $AFMCP_N$ strain, which carries a P_N::lacZ translational fusion integrated into its chromosome (Table 1) and would be expected to lack a histidine kinase capable of phosphorylating AccR. Similar activities from the P_N promoter were found in *E. coli* $AFMCP_N$ harbouring either a vector control or a plasmid expressing AccR, while P_N activity was reduced ~4-fold in the strain harbouring a plasmid expressing AccRD60E (Fig. 7*A*).

The results outlined above demonstrate that the unphosphorylated AccRD60E protein is able to effectively bind and repress P_N promoter activity in *E. coli*. To test if this was also the case in *Azoarcus* sp. CIB, we monitored the effect of expressing AccRD60E on the ability of the AccR null strain to grow anaerobically at the expense of benzoate. Whereas *Azoarcus* sp. CIBΔ*accR* was able to grow on benzoate (Fig. 7*B*, triangles), *Azoarcus* sp. CIBΔ*accR* harbouring a plasmid expressing AccRD60E protein could not (Fig. 7*B*, squares). These results strongly support the idea that AccRD60E is constitutively active in *Azoarcus* and behaves as a super-repressor of the *bzd* cluster through inhibiting the activity of the P_N promoter.

AccR Is a Master Regulator Controlling All Central Pathways for the Anaerobic Catabolism of Aromatics in Azoarcus sp. CIB-In addition to the *bzd*-pathway, the *Azoarcus* sp. CIB *mbd* pathway for anaerobic assimilation of 3-methylbenzoate/*m*-xylene is also subject to CCR control in response to some organic acids (34). To explore whether AccR also controls expression of the *mbd* genes, we monitored the activity of the P_{B1} promoter that drives expression of the *mbd* genes using a P_{B1}::*lacZ* translational fusion reporter plasmid. While succinate caused inhibition of P_{B1} promoter activity in the wild-type CIB strain, no inhibition of P_{B1} activity was observed in the AccR null strain (Fig. 8*A*). A direct interaction between AccR-P with the P_{B1} promoter was confirmed by gel-retardation (Fig. 8*B*). Taken together, these results demonstrated that AccR is also involved in succinate mediated anaerobic CCR control of the *mbd* genes in *Azoarcus* sp. CIB.

A third distinct central pathway for anaerobic degradation of aromatics in

Azoarcus sp. CIB is the *hbd*-pathway devoted to 3-hydroxybenzoate catabolism (22). To determine whether AccR also controls the expression of the genes for 3-hydroxybenzoate catabolism, *Azoarcus* sp. CIBΔ*accR* harbouring a plasmid expressing wild type AccR or AccRD60E were grown anaerobically in minimal medium containing 3-hydroxybenzoate as the sole carbon source. As was the case for growth at the expense of benzoate (Fig. 7*B*), cells expressing AccR were able to grow on 3-hydroxybenzoate whilst those expressing the constitutively active AccRD60E super-repressor could not. Hence, these results strongly suggests that the genes responsible of the anaerobic catabolism of 3-hydroxybenzoate are also negatively controlled by AccR. Together with the impact of AccR on the *bzd*- and *mbd*-pathways, the results provide additional support for the idea that AccR is a master regulator of the anaerobic catabolism of aromatic compounds in *Azoarcus* sp. CIB.

The AccR-Mediated CCR Control is Only Operational under Anaerobic Growth Conditions-To explore whether AccR also mediates CCR control of aerobic degradation of aromatic compounds, we used real-time RT-PCR to monitor the activity of the P_D promoter, which drives the expression of the *box* genes for the aerobic degradation of benzoate in *Azoarcus* sp. CIB (27). When the cells were grown aerobically in benzoate, succinate significantly inhibited the activity of P_D promoter; however, this inhibition was not attributable to AccR since it was also observed in the AccR null strain (Fig. 9*A*). Since we have shown previously that the *box* genes can be also expressed under anaerobic growth conditions (27), we tested whether such anaerobic expression was controlled by AccR. In contrast to the results obtained under aerobic growth conditions, when the cells were grown anaerobically in the presence of benzoate, succinate-mediated inhibition was found in the wild-type but not the AccR null strain (Fig. 9*B*). As is the case for the P_N and P_{B1} promoters, the P_D promoter was bound by AccR-P in gel-retardation assays (Fig. 9*C*) and also contains a sequence that bears homology to the ATGCA-N_6-TGCAT motif identified on the basis of AccR-P binding to P_N (Fig. 9D). Taken together these results indicate that the AccR regulatory circuit operates through binding to common DNA motifs and is only operational under anaerobic growth conditions.

DISCUSSION

When faced with a mixture of alternative carbon sources, bacteria usually strategically utilize the substrate that yields the highest energy return. The utilization of preferred carbon sources is controlled by global regulatory mechanisms, termed CCR, which depends on the energy status of the cell and that also responds to other environmental conditions, such as growth temperature and carbon source concentrations, thus conferring to the bacteria with a competitive advantage in natural environments (4,52,53). Aromatic compounds usually constitute a secondary (non preferred) carbon source for many bacteria. Diverse mechanisms underlie CCR control in aerobic metabolism of aromatic compounds (6-11, 16-18). Here we report the first known mechanism that accounts for CCR control of anaerobic catabolism of aromatic compounds in bacteria – namely the transcriptional repressor AccR of *Azoarcus* sp. CIB. Our evidence that AccR can be considered as a master regulator of anaerobic catabolism of aromatics is based on the finding that this protein controls expression of all known central anaerobic aromatic catabolic pathways of this strain. These include the *bdz*-pathway for dissimilation of benzoate, the 3-methybenzoate *mbd*-pathway, the 3-hydroxybenzoate *hbd*-pathway, and the benzoate *box*-pathway as expressed under anaerobic growth conditions (Figs. 1, 4*F*, 8, 9). Because expression of the *box*-pathway is only affected by the lack of AccR under anaerobic but not aerobic conditions (Fig. 9), we suggest that the AccR circuitry is only operational under anaerobic growth conditions.

In silico analysis assigns AccR to the FixJ/NarL family of response regulators (Supplemental Fig. S1) whose members participate in the control of a wide variety of biological functions (45-47). We found

that, like some previously characterised members of this family [e.g. FixJ, OmpR, PhoB and StyR (54-56)], phosphorylation of AccR to AccR-P with high-energy small molecule phosphodonors (e.g., carbamoyl phosphate) (Fig. 2*B*) triggers a monomer-to-dimer transition (Fig. 2*D* and *E*); however, this reconfiguration does not change the apparent overall elongated shape of the AccR protomers. Under our *in vitro* conditions, only ~50% phosphorylation of AccR was achieved (Fig. 2*B* and *D*). This could be attributable to partial phosphorylation or spontaneous dephosphorylation; alternatively, it may be due to an innate phosphatase activity of AccR. In this respect, it is well established that despite extensive structural and chemical similarities, the half life of the phosphorylated state of response regulators varies extensively (from seconds to hours) depending on both their innate auto-phosphorylation and auto-dephosphorylation kinetics (42).

In addition to subunit configuration, phosphorylation controls the ability of AccR to bind DNA (Fig. 3) and its capacity to cause repression of promoter output in *in vitro* transcription assays (Fig. 5). Conversely, substitution of the highly conserved Asp^{60} residue of the N-terminal REC motif of AccR to a phosphor-mimic Glu residue (AccRD60E) renders the protein constitutively active (phosphorylation-independent) both in terms of its DNA binding ability (Fig. 3*C*) and its capacity to repress promoter output in intact cells (Fig. 7), suggesting that Asp^{60} is the target residue of phosphorylation. Thus, AccR behaves like a typical response regulator that upon activation represses promoter output both *in vivo* and *in vitro*. The lack of anaerobic growth in benzoate of an AccR null derivative of *Azoarcus* sp. CIB expressing the AccRD60E protein (Fig. 7*B*), is consistent with the role of this mutant regulator as a super-repressor of the *bzd* central pathway.

The phosphorylation-triggered monomer-to-dimer transition of AccR suggests that the AccR-P would bind DNA as a dimer – a configuration consistent with our identification of the inverted repeat ATGCA-N_6-TGCAT as the AccR DNA binding site within the P_N promoter. The P_N promoter harbours two of these sites (denoted OR1 and OR2) which can each be bound independently by AccR with approximately equal affinity (Fig. 4), while the P_{B1} and P_D promoters, which are also targeted by AccR (Figs. 8 and 9), possess one copy of this motif (Fig. 9D). A truncated P_N promoter that lacks the AccR binding regions (P_{N1}) did not show succinate dependent CCR control (Fig. 4*F*), which illustrates how a rational design of a target promoter can be an interesting strategy to circumvent CCR in bacteria. The location of the AccR binding region within P_N (spanning position -35 to -153 relative to the transcriptional start site) is consistent with the observed repressor role of AccR. We can envisage two plausible and non-mutually exclusive means by which DNA binding by AccR-P could inhibit promoter output: i) inhibition of closed complex formation by occluding RNA polymerase and/or ii) inhibition of open complex formation by preventing binding of the AcpR activator whose operator region spans from -42.5 to -39.5 (25).

In contrast to the apparent dimerization-dependent DNA-binding of intact AccR-P, the DNA-binding proficient C-terminal domain of AccR (CAccR) is monomeric in solution (Fig. 6). These findings suggest that i) dimerization *per se* is not a prerequisite for DNA binding, and ii) that dimerization is carried out through the N-terminal domain, as exemplified by NarL (46). Further, the results suggest a regulatory scenario in which phosphorylation of Asp^{60} of AccR alleviates inter-domain repression mediated by the N-terminal domain to allow reconfiguration to a DNA-binding proficient configuration. Since linker regions can be crutial for correct inter-domain communication (57), it is plausable that the long linker region of AccR may play a role in transmitting the phosphorylation-dependent conformational changes (from the NAccR domain to the CAccR domain) to result in de-repression and thus activation of its capacity to bind to target promoters. However, like a potential auto-phosphatase activity of AccR, these mechanistic possibilities require experimental verification.

As described in the introduction, amongst the diverse proteins that have been

found to be involved in CCR control of aerobic catabolism of aromatic compounds, only one – BphQ – is a response regulator. A search of *accR* homologs in bacterial genomes revealed the presence of AccR-like proteins (amino acid sequence identity higher than 70%) encoded in the genomes of other *Azoarcus* and *Thauer*a strains (Supplemental Fig. S1*A*). These AccR-like regulators cluster in a branch of the phylogenetic tree different to that of the BphQ-like regulators (Supplemental Fig. S1*B*), which suggests that both types of proteins, although evolutionary related, constitute different sub-groups of response regulators. In this respect it is worth noting that AccR from *Azoarcus* sp. CIB and BphQ from *Acidovorax* sp. KKS102 have completely different regulatory features: whereas BphQ is a transcriptional activator that binds its target DNA in the absence of phosphorylation (7), AccR is a repressor that requires phosphorylation in order to bind to a target operator that is completely different to that described for BphQ.

Many *β*-proteobacteria *Azoarcus* and *Thauera* strains are able to anaerobically metabolise aromatic compounds. The presence of *accR* orthologs within their genomes raises the possibility that AccR constitutes a new global regulator that controls anaerobic carbon catabolite repression in this group of organisms. Our observation that the *accR*-genes are always located adjacent to a gene that encodes a putative sensor histidine kinase strongly suggests that the latter would be responsible for maintaining AccR in its active phosphorylated state in the presence of preferred carbon sources such as succinate. The work presented here should greatly facilitate our future efforts aimed to characterize this predicted two-component regulatory system and to decipher the environmental signals that trigger the activation/inactivation status of AccR.

Acknowledgments-The technical work of A. Valencia is greatly appreciated. The assistance of Secugen S.L. with DNA sequencing, that of C.A. Botello/J.R. Luque with ultracentrifugation experiments, and of V. de los Ríos with the MALDI-TOF analyses, are gratefully acknowledged. The authors are grateful to G. Durante-Rodríguez for providing plasmid pBBR5P$_{NI}$.

REFERENCES

1. Görke, B., and Stülke, J. (2008) Carbon catabolite repression in bacteria: many ways to make the most out of nutrients. *Nat. Rev. Microbiol.* **6**, 613-624
2. Collier, D.N., Hager, P.W., and Phibbs, P.V., Jr. (1996) Catabolite repression control in the Pseudomonads. *Res. Microbiol.* **147**, 551-561
3. Moreno, R., Fonseca, P., and Rojo, F. (2012) Two small RNAs, CrcY and CrcZ, act in concert to sequester the Crc global regulator in *Pseudomonas putid*a, modulating catabolite repression. *Mol. Microbiol.* **83**, 24-40
4. Rojo, F. (2010) Carbon catabolite repression in *Pseudomonas*: optimizing metabolic versatility and interactions with the environment. *FEMS Microbiol. Rev.* **34**, 658-684
5. Shingler, V. (2003) Integrated regulation in response to aromatic compounds: from signal sensing to attractive behaviour. *Environ. Microbiol.* **5**, 1226-1241
6. Marqués, S., Aranda-Olmedo, I., and Ramos, J.L. (2006) Controlling bacterial physiology for optimal expression of gene reporter constructs. *Curr. Opin. Biotechnol.* **17**, 50-56
7. Ohtsubo, Y., Goto, H., Nagata, Y., Kudo, T., and Tsuda, M. (2006) Identification of a response regulator gene for catabolite control from a PCB-degrading beta-proteobacteria, *Acidovorax* sp. KKS102. *Mol. Microbiol.* **60**, 1563-1575
8. Prieto, M.A., Galán, B., Torres, B., Ferrández, A., Fernández, C., Miñambres, B., García, J.L., and Díaz, E. (2004) Aromatic metabolism versus carbon availability: the regulatory network that controls catabolism of less-preferred carbon sources in *Escherichia coli*. *FEMS Microbiol. Rev.* **28**, 503-518
9. Morales, G., Linares, J.F., Beloso, A., Albar, J.P., Martínez, J.L., and Rojo, F. (2004) The *Pseudomonas putida* Crc global regulator controls the expression of genes from several chromosomal catabolic pathways for aromatic compounds. *J. Bacteriol.* **186**, 1337-1344
10. Moreno, R., Fonseca, P., and Rojo, F. (2010) The Crc global regulator inhibits the *Pseudomonas putida* pWW0 toluene/xylene assimilation pathway by repressing the translation of regulatory and structural genes. *J. Biol. Chem.* **285**, 24412-24419
11. Hernández-Arranz, S., Moreno, R., and Rojo, F. (2013) The translational repressor Crc controls the *Pseudomonas putida* benzoate and alkane catabolic pathways using a multi-tier regulation strategy. *Environ. Microbiol.* **15**, 227-241
12. MacGregor, C.H., Wolff, J.A., Arora, S.K., and Phibbs, P.V (1991) Cloning of a catabolite repression control (*crc*) gene from *Pseudomonas aeruginosa*, expression of the gene in *Escherichia coli*, and identification of the gene product in *Pseudomonas aeruginosa*. *J. Bacteriol.* **173**, 7204-7212
13. Moreno, R., Martínez-Gomariz, M., Yuste, L., Gil, C., and Rojo, F. (2009) The *Pseudomonas putida* Crc global regulator controls the hierarchical assimilation of amino acids in a complete medium: evidence from proteomic and genomic analyses. *Proteomics* **9**, 2910-2928
14. Hester, K.L., Madhusudhan, K.T., and Sokatch, J.R. (2000) Catabolite repression control by *crc* in 2xYT medium is mediated by posttranscriptional regulation of *bkdR* expression *in Pseudomonas putida*. *J. Bacteriol.* **182**, 1150-1153
15. Milojevic, T., Grishkovskaya, I., Sonnleitner, E., Djinovic-Carugo, K., and Blasi, U. (2013) The *Pseudomonas aeruginosa* catabolite repression control protein Crc is devoid of RNA binding activity. *PloS One* **8**, e64609
16. Pflüger, K., and de Lorenzo, V. (2008) Evidence of in vivo cross talk between the nitrogen-related and fructose-related branches of the carbohydrate phosphotransferase system of *Pseudomonas putida*. *J. Bacteriol.* **190**, 3374-3380
17. Morales, G., Ugidos, A., and Rojo, F. (2006) Inactivation of the *Pseudomonas putida* cytochrome o ubiquinol oxidase leads to a significant change in the transcriptome and to increased expression of the CIO and cbb3-1 terminal oxidases. *Environ. Microbiol.* **8**, 1764-1774

18. Petruschka, L., Burchhardt, G., Muller, C., Weihe, C., and Herrmann, H. (2001) The *cyo* operon of *Pseudomonas putida* is involved in carbon catabolite repression of phenol degradation. *Mol. Genet. Genomics* **266**, 199-206
19. Heider, J., Boll, M., Breese, K., Breinig, S., Ebenau-Jehle, C., Feil, U., Gad'on, N., Laempe, D., Leuthner, B., Mohamed, M.E. *et al.* (1998) Differential induction of enzymes involved in anaerobic metabolism of aromatic compounds in the denitrifying bacterium *Thauera aromatica*. *Arch. Microbiol.* **170**, 120-131
20. López-Barragán, M.J., Carmona, M., Zamarro, M.T., Thiele, B., Boll, M., Fuchs, G., García, J.L., and Díaz, E. (2004) The *bzd* gene cluster, coding for anaerobic benzoate catabolism, in *Azoarcus* sp. strain CIB. *J. Bacteriol.* **186**, 5762-5774
21. Trautwein, K., Grundmann, O., Wohlbrand, L., Eberlein, C., Boll, M., and Rabus, R. (2011) Benzoate mediates repression of C(4)-dicarboxylate utilization in "*Aromatoleum aromaticum*" EbN1. *J. Bacteriol.* **194**, 518-528
22. Carmona, M., Zamarro, M.T., Blázquez, B., Durante-Rodríguez, G., Juárez, J.F., Valderrama, J.A., Barragán, M.J., García, J.L., and Díaz, E. (2009) Anaerobic catabolism of aromatic compounds: a genetic and genomic view. *Microbiol. Mol. Biol. Rev*. **73**, 71-133
23. Barragán, M.J.L., Blázquez, B., Zamarro, M.T., Mancheño, J.M., García, J.L., Díaz, E., and Carmona, M. (2005) BzdR, a repressor that controls the anaerobic catabolism of benzoate in *Azoarcus* sp. CIB, is the first member of a new subfamily of transcriptional regulators. *J. Biol. Chem.* **280**, 10683-10694
24. Durante-Rodríguez, G., Valderrama, J.A., Mancheño, J.M., Rivas, G., Alfonso, C., Arias-Palomo, E., Llorca, O., García, J.L., Díaz, E., and Carmona, M. (2010) Biochemical characterization of the transcriptional regulator BzdR from *Azoarcus* sp. CIB. *J. Biol. Chem.* **285**, 35694-35705
25. Durante-Rodríguez, G., Zamarro, M.T., García, J.L., Díaz, E., and Carmona, M. (2006) Oxygen-dependent regulation of the central pathway for the anaerobic catabolism of aromatic compounds in *Azoarcus* sp. strain CIB. *J. Bacteriol.* **188**, 2343-2354
26. Durante-Rodríguez, G., Zamarro, M.T., García, J.L., Díaz, E., and Carmona, M. (2008) New insights into the BzdR-mediated transcriptional regulation of the anaerobic catabolism of benzoate in *Azoarcus* sp. CIB. *Microbiology* **154**, 306-316
27. Valderrama, J.A., Durante-Rodríguez, G., Blázquez, B., García, J.L., Carmona, M., and Díaz, E. (2012) Bacterial degradation of benzoate: cross-regulation between aerobic and anaerobic pathways. *J. Biol. Chem.* **287,** 10494-10508
28. Casadaban, M.J. (1976) Transposition and fusion of the *lac* genes to selected promoters in *Escherichia coli* using bacteriophage *lambda* and *Mu*. *J. Mol. Biol.* **104**, 541-555
29. Miller, V.L., and Mekalanos, J.J. (1988) A novel suicide vector and its use in construction of insertion mutations: osmoregulation of outer membrane proteins and virulence determinants in *Vibrio cholerae* requires *toxR*. *J. Bacteriol.* **170**, 2575-2583
30. de Lorenzo, V., and Timmis, K.N. (1994) Analysis and construction of stable phenotypes in gram-negative bacteria with Tn*5*- and Tn*10*-derived minitransposons. *Methods Enzymol*. **235**, 386-405
31. Kaniga, K., Delor, I., and Cornelis, G.R. (1991) A wide-host-range suicide vector for improving reverse genetics in gram-negative bacteria: inactivation of the *blaA* gene of *Yersinia enterocolitica*. *Gene* **109**, 137-141
32. Moreno-Ruíz, E., Hernáez, M.J., Martínez-Perez, O., and Santero, E. (2003) Identification and functional characterization of *Sphingomonas macrogolitabida* strain TFA genes involved in the first two steps of the tetralin catabolic pathway. *J. Bacteriol.* **185**, 2026-2030
33. Kovach, M.E., Elzer, P.H., Hill, D.S., Robertson, G.T., Farris, M.A., Roop, R.M.I., and Peterson, K.M. (1995) Four new derivatives of the broad-host-range cloning vector pBBR1MCS, carrying different antibiotic-resistance cassettes. *Gene* **166**, 175-176
34. Juárez, J.F., Zamarro, M.T., Eberlein, C., Boll, M., Carmona, M., and Díaz, E. (2013) Characterization of the *mbd* cluster encoding the anaerobic 3-methylbenzoyl-CoA central pathway. *Environ. Microbiol.* **15**, 148-166

35. Sambrook, J., and Rusell D. W. (2001) *Molecular cloning: A laboratory manual*, 3rd. Ed., Cold Spring Harbor laboratory, Cold Spring Harbor, NY
36. Miller, J.H. (1972). *Experiments in Molecular Genetics*, Cold Spring Harbor Laboratory, Cold Spring Harbor, NY
37. Thompson, J.D., Higgins, D.G., and Gibson, T.J. (1994) CLUSTAL W: improving the sensitivity of progressive multiple sequence alignment through sequence weighting, position-specific gap penalties and weight matrix choice. *Nucleic Acids Res.* **22**, 4673-4680
38. Kimura, M. (1980) A simple method for estimating evolutionary rates of base substitutions through comparative studies of nucleotide sequences. *J. Mol. Evol.* **16**, 111-120
39. Saitou, N., and Nei, M. (1987) The neighbor-joining method: a new method for reconstructing phylogenetic trees. *Mol. Biol. Evol.* **4**, 406-425
40. Felsenstein, J. (1993) PHYLYP (*Phylogenetic Inference Package*) Version 3.5.1. Department of Genetics, University of Washington, Seattle, WA
41. Schuck, P. (2000) Size-distribution analysis of macromolecules by sedimentation velocity ultracentrifugation and lamm equation modeling. *Biophys. J.* **78**, 1606-1619
42. Laue, T.M., Shah, B. D., Ridgeway, T. M., and Pelletier, S. L. (1992) *Analytical ultracentrifugation in biochemistry*. Royal Society of Chemistry, Cambridge, UK.
43. Maxam, A.M., and Gilbert, W. (1980) Sequencing end-labeled DNA with base-specific chemical cleavages. *Methods Enzymol.* **65**, 499-560
44. Kiley, P.J., and Reznikoff, W.S. (1991) Fnr mutants that activate gene expression in the presence of oxygen. *J. Bacteriol.* **173**, 16-22
45. Kurashima-Ito, K., Kasai, Y., Hosono, K., Tamura, K., Oue, S., Isogai, M., Ito, Y., Nakamura, H., and Shiro, Y. (2005) Solution structure of the C-terminal transcriptional activator domain of FixJ from *Sinorhizobium meliloti* and its recognition of the *fixK* promoter. *Biochemistry* **44**, 14835-14844
46. Maris, A.E., Sawaya, M.R., Kaczor-Grzeskowiak, M., Jarvis, M.R., Bearson, S.M., Kopka, M.L., Schroder, I., Gunsalus, R.P., and Dickerson, R.E. (2002) Dimerization allows DNA target site recognition by the NarL response regulator. *Nat. Struct. Biol.* **9**, 771-778
47. Milani, M., Leoni, L., Rampioni, G., Zennaro, E., Ascenzi, P., and Bolognesi, M. (2005) An active-like structure in the unphosphorylated StyR response regulator suggests a phosphorylation- dependent allosteric activation mechanism. *Structure* **13**, 1289-1297
48. Bourret, R.B. (2010) Receiver domain structure and function in response regulator proteins. *Curr. Opin. Microbiol.* **13**, 142-149
49. Klose, K.E., Weiss, D.S., and Kustu, S. (1993) Glutamate at the site of phosphorylation of nitrogen-regulatory protein NTRC mimics aspartyl-phosphate and activates the protein. *J. Mol. Biol.* **232**, 67-78
50. Lan, C.Y., and Igo, M.M. (1998) Differential expression of the OmpF and OmpC porin proteins in *Escherichia coli* K-12 depends upon the level of active OmpR. *J. Bacteriol.* **180**, 171-174
51. Gao, R., and Stock, A.M. (2010) Molecular strategies for phosphorylation-mediated regulation of response regulator activity. *Curr. Opin. Microbiol.* **13**, 160-167
52. Fonseca, P., Moreno, R., and Rojo, F. (2012) *Pseudomonas putida* growing at low temperature shows increased levels of CrcZ and CrcY sRNAs, leading to reduced Crc-dependent catabolite repression. *Environ. Microbiol.* **15**, 24-35
53. Valentini, M., and Lapouge, K. (2013) Catabolite repression in *Pseudomonas aeruginosa* PAO1 regulates the uptake of C4 -dicarboxylates depending on succinate concentration. *Environ. Microbiol.* **15**, 1707-1716
54. Da Re, S., Schumacher, J., Rousseau, P., Fourment, J., Ebel, C., and Kahn, D. (1999) Phosphorylation-induced dimerization of the FixJ receiver domain. *Mol. Microbiol.* **34**, 504-511

55. Leoni, L., Ascenzi, P., Bocedi, A., Rampioni, G., Castellini, L., and Zennaro, E. (2003) Styrene-catabolism regulation in *Pseudomonas fluorescens* ST: phosphorylation of StyR induces dimerization and cooperative DNA-binding. *Biochem. Biophys. Res. Commun.* **303**, 926-931
56. Bachhawat, P., Swapna, G.V., Montelione, G.T., and Stock, A.M. (2005) Mechanism of activation for transcription factor PhoB suggested by different modes of dimerization in the inactive and active states. *Structure* **13**, 1353-1363
57. Mattison, K., Oropeza, R., and Kenney, L.J. (2002) The linker region plays an important role in the interdomain communication of the response regulator OmpR. *J. Biol. Chem.* **277**, 32714-32721

FIGURE LEGENDS

FIGURE 1**. The *accR* gene is required for CCR control of the P_N promoter.** *Azoarcus* sp. CIB (CIB), its AccR null counterpart (CIBΔ*accR*), and CIBΔ*accR* harbouring plasmid pBBR5AccR that expresses AccR from the *Plac* promoter (CIBΔ*accR/accR*), were grown anaerobically in minimal medium supplemented with 3 mM benzoate (*black bars*) or a mixture of 3 mM benzoate and 0.4% succinate (*white bars*). Total RNA was isolated from cells grown until mid-exponential phase and the activity of the P_N promoter (in arbitrary units) was measured by real-time RT-PCR. Graphed values are the average of three independent experiments +/- S.D.

FIGURE 2**. *In vitro* phosphorylation of AccR provokes a monomer-to-dimer transition.** *A* and *B***,** mass spectrometry (MALDI-TOF) of untreated His_6-AccR (*panel A)* and His_6-AccR preincubated with 20 mM carbamoyl phosphate (*panel B*). Molecular masses of the peaks corresponding to unphosphorylated (AccR) and phosphorylated (AccR-P) proteins are indicated. *C* and *D***,** sedimentation coefficient distribution c(s) corresponding to 10 μM untreated His_6-AccR (*panel C*) and carbamoyl phosphate treated His_6-AccR (*panel D*) are represented in relation to the sedimentation coefficient (*S*). The peaks corresponding to the AccR and AccR-P species are indicated. The *s* value of the proteins did not change significantly with protein concentration over the range examined (5-40 μM). *E***,** sedimentation equilibrium data of untreated (*squares*) and carbamoyl phosphate treated His_6-AccR (*circles*). Best fit analysis assuming a theoretical protein monomer (*solid line*) or dimer (*dashed line*) is also shown.

FIGURE 3**. DNA binding by AccR is phosphorylation dependent.** Gel-retardation analyses of the P_N probe by AccR derivatives (0 to 12 μM) as described under "Experimental Procedures". *A*, assays with increasing concentrations of untreated His_6-AccR protein (AccR). Free P_N probe is indicated by an *arrow*. *B*, assays performed with increasing concentrations of carbamoyl phosphate treated His_6-AccR (AccR-P). Free P_N probe and the major P_N/AccR-P complex are indicated by *arrows*. *C***,** assays performed with increasing concentrations of His_6-AccRD60E (AccRD60E). Free P_N probe and the major P_N/AccRD60E complex are indicated by *arrows*.

FIGURE 4**. AccR-P binds to two palindromic operator sequences within the P_N promoter.** *A*, DNase I footprinting analyses of the P_N probe with 0 to 12 μM carbamoyl phosphate treated His_6-AccR (AccR-P) as described under "Experimental Procedures". *Lane AG* shows an A+G Maxam and Gilbert sequencing reaction with the location of the -10 and -35 boxes and the transcription initiation site (+1) indicated *to the left*. The AccR-P protected region between positions -153 and -34 is highlighted by a *bracket*, with phosphodiester bonds mildly hypersensitive to DNase I cleavage indicated by *asterisks*. *B***,** expanded view of the P_N promoter sequence. Inferred -10 and -35 promoter elements and the transcription start site (+1) are indicated *in italics*. The ribosome-binding site (RBS) and the *bzdN* ATG initiation codon are *underlined*. The region protected by AccR-P (as under *panel A*) is *boxed* with the location of the palindrome operator sequences (OR1 and OR2) indicated by *convergent arrows*. Nucleotides corresponding to the P_{N2} and P_{N3} probes used in *panels C* and *D* are *underlined with discontinuous and continuous lines*, respectively. *C* to *E***,** gel-retardation analyses of the indicated probes as under Fig. 3*B*. Gel-retardation assays were performed using increasing concentrations (0 to 12 μM) of carbamoyl phosphate treated His_6-AccR (AccR-P). The free probes and the major DNA/AccR-P complexes are indicated by *arrows*. *F*, effect of succinate on the activity of the native P_N promoter and the truncated P_{NI} promoter that lacks the OR1 and OR2 operators. *Azoarcus* sp. CIB cells harbouring the *P_N::lacZ* translational reporter plasmid $pBBR5P_N$ or the *P_{NI}::lacZ* translational reporter plasmid $pBBR5P_{NI}$ were grown anaerobically in minimal medium containing 3 mM benzoate (*black bars*) or a mixture of 3 mM benzoate and 0.2% succinate (*white bars*) until the mid-exponential phase. Values are the average of three independent experiments +/- S.D, and are graphed setting the β-galactosidase activities obtained

for each promoter in the absence of succinate (22000 and 2500 Miller units for P_N and P_{NI}, respectively) as 100%.

FIGURE 5. **AccR-P represses transcription from the P_N promoter *in vitro*.** Multiple-round *in vitro* transcription reactions, as detailed in "Experimental Procedures", contained 5 nM of supercoiled pJCD-P_N plasmid DNA (which produces a 184-nucleotide mRNA from P_N and a 105-nucleotide control mRNA), 40 nM of *E. coli* RNA polymerase, and 200 nM of the His_6-Fnr* activator. Reactions were carried out in the absence of AccR, or in the presence of increasing concentrations of phosphorylated His_6-AccR (AccR-P) or unphosphorylated His_6-AccR (AccR).

FIGURE 6. **CAccR functions as an independent monomeric DNA binding domain.** *A*, gel retardation analysis of the P_N probe, as under Fig. 3*A*, using increasing concentrations (0 to 10 μM) of His_6-CAccR (CAccR). The free P_N probe and the major P_N/CAccR complex are indicated by *arrows*. *B*, sedimentation coefficient distribution c(s) corresponding to 10 μM His_6-CAccR is represented in relation to the sedimentation coefficient (*S*). The peak corresponding to the single His_6-CAccR species detected is indicated. *C*, sedimentation equilibrium data of His_6-CAccR (*circles*) and best fit analysis assuming a theoretical protein monomer (*solid line*) or dimer (*dashed line*).

FIGURE 7. **The AccRD60E protein acts as a constitutive repressor of the P_N promoter.** *A*, effect of the AccRD60E protein on the activity of the P_N promoter in *E. coli* AFMCP_N cells that contain a chromosomal P_N::*lacZ* fusion. Cells harbouring a plasmid expressing the AccRD60E (pIZAccRD60E), AccR (pIZAccSR), or a cognate vector control (C, pIZ1016), were grown anaerobically in glycerol-containing minimal medium until mid-exponential phase. Graphed values of β-galactosidase activities (in Miller units) are the average from three independent experiments +/- S. D. *B*, anaerobic growth of *Azoarcus* sp. CIBΔ*accR* (*triangles*) and *Azoarcus* sp. CIBΔ*accR* harbouring pIZAccRD60E (*squares*) in minimal medium containing 3 mM benzoate as the sole carbon source.

FIGURE 8. **AccR controls the activity of the P_{B1} promoter**. *A*, *Azoarcus* sp. CIB (CIB) and *Azoarcus* sp. CIBΔ*accR* (CIBΔ*accR*) cells harbouring the P_{B1}::*lacZ* reporter plasmid pIZP_{B1} were grown anaerobically in minimal medium containing a mixture of 3 mM 3-methylbenzoate and 1 mM benzoate as a co-carbon source that does not cause CCR of the P_{B1} promoter (*black bars*), or in minimal medium containing a mixture of 3 mM 3-methylbenzoate and 0.2 % succinate as a co-carbon source that causes CCR of the P_{B1} promoter (*white bars*). Values are the average of three independent experiments +/- S. D. obtained for cells grown to the mid-exponential phase. *B*, gel retardation analyses of P_{B1} probe as under Fig. 3*B*. Assays were performed using increasing concentrations (0 to 12 μM) of carbamoyl phosphate treated His_6-AccR (AccR-P). The free P_{B1} probe and the major P_{B1}/AccR-P complex are indicated by *arrows*.

FIGURE 9. **AccR controls the activity of the P_D promoter under anaerobic conditions**. *A* and *B*, *Azoarcus* sp. CIB (CIB) and *Azoarcus* sp. CIBΔ*accR* (CIBΔ*accR*) cells were grown aerobically (*panel A*) or anaerobically (*panel B*) in minimal medium containing 3 mM benzoate (*black bars*) or a mixture of 3 mM benzoate and 0.2% succinate (*white bars*) until mid-exponential phase. Transcripts from the P_D promoter were measured by real-time RT-PCR. Graphed values (in arbitrary units) are the average from three independent experiments +/- S. D. *C*, gel retardation analyses of P_D probe as under Fig. 3*B*. Assays were performed at increasing concentrations (0 to 12 μM) of carbamoyl phosphate treated His_6-AccR (AccR-P). The free P_D probe and the major P_D/AccR-P complex are indicated by *arrows*. *D*, sequence alignment of AccR binding regions in different catabolic promoters of *Azoarcus* sp. CIB. P_N (OR2), operator region 2 of the P_N promoter; P_N (OR1), operator region 1 of the P_N promoter; P_D, P_D promoter of the *box* cluster; P_{B1}, P_{B1} promoter of the *mbd* cluster. A consensus sequence of the AccR operator is shown *at the bottom*. Nucleotides identical to the consensus are shown in *bold*.

TABLE 1
Bacterial strains and plasmids used in this study

Strain or plasmid	Relevant genotype or phenotype[a]	Ref. or source
***E. coli* strains**		
DH10B	F´, *mcrA* Δ(*mrr hsdRMS-mcrBC*) ϕ80d*lac*ΔM15 Δ*lacX74 deoR recA1 araD139* Δ(*ara-leu*)*7697 galU galK rpsL* (Sm^r) *endA1 nupG*	Invitrogen
M15	Strain for regulated high level expression with pQE vectors	Qiagen
MC4100	*araD139* Δ(*argF-lac*)U169 *rpsL*150 (Sm^r) *relA1 flbB*5301 *deo*C1 *ptsF25 rbsR*	28
$AFMCP_N$	Km^r Rf^r, MC4100 spontaneous rifampicin-resistant mutant harboring a chromosomal insertion of the P_N*::lacZ* translational fusion	23
SM10 λ*pir*	Km^r *thi-1 thr leu tonA lacY supE recA*::RP4-2-Tc::Mu λ*pir* lysogen	29
S17-1λ*pir*	Tp^r Sm^r *recA thi hsdRM*$^+$ RP4::2-Tc::Mu::Km Tn*7* λ*pir* lysogen	30
XLI-Bue MRA (P2)	Δ(*mcrA*)183, Δ(*mcrCB-hsdSMR-mrr*)173, *endA1*, *gyrA96*, *supE44*, *relA1*, *thi-1*, *lac*, P2 lysogen	Stratagene
***Azoarcus* sp.CIB strains**		
CIB	Wild type strain	20
CIBΔ*accR*	*Azoarcus* sp. strain CIB with a deletion of the *accR* gene	This work
Plasmids		
pQE32	Ap^r, *ori*ColE1, T5 promoter *lac* operator, λ t_o*/E. coli rrnB T1* terminators, N-terminal His_6	Qiagen
pQE32-His_6AccR	Ap^r, pQE32 derivative for expression of His_6-*accR;* carries a 636 bp BamHI to PstI fragment generated using primers 5'HisaccR and 3'HisaccR (Table 2)	This work
pQE32-His_6CAccR	Ap^r, pQE32 derivative for expression of His_6-*CaccR;* carries a 232-bp BamHI to PstI fragment generated using 5'HisCaccR and 3'HisaccR (Table 2)	This work
pQE32- His_6AccRD60E	Ap^r, pQE32 derivative for expression of His_6- *accRD60E;* carries a 636 bp BamHI to PstI fragment generated using flanking primers 5'HisaccR and 3'HisaccR and overlapping PCR mutagenesis primers 5´AccRD60E and 3´AccRD60E.	This work
pREP4	Km^r, plasmid that expresses the *lacI* repressor	Qiagen
pECOR7	Ap^r, pUC19 harbouring a 7.1 kb EcoRI fragment containing the *bzdRNO* genes	20
pKNG101	Sm^r, *ori*R6K, Mob^+. Suicide vector with a *sacB* selection marker for gene replacement by double site homologous recombination	31
pKNG101ΔaccR	Sm^r, pKNG101 derivative carrying the Δ*accR* allele as a 1.4 kb BamHI to SpeI fragment assembled using the four AccRmut primers listed in Table 2	This work
pIZ1016	Gm^r, *ori*pBBR1, Mob^+, *lacZ*α, *Ptac*/*lacI*^{q}, broad-host-range cloning and expression vector	32
pIZAccSR	Gm^r, pIZ1016 derivative expressing *accR* from the *Ptac* promoter; carries a 3.3 kb SalI to SpeI fragment amplified using primers 5'AccSR and 3'AccSR (Table 2)	This work
pIZAccRD60E	Gm^r, pIZ1016 derivative expressing the His_6-*accRD60E* from the *Ptac* promoter; carries a 0.6 kb BamHI to PstI fragment derived from pQE32- His_6AccRD60E	This work
pBBR1MCS-5	Gm^r, *ori*pBBR1, Mob^+, *lacZ*α, *Plac*, broad-host-range cloning and expression vector	33
pBBR5AccR	Gm^r, pBBR1MCS-5 derivative expressing the *accR* gene from the *Plac* promoter; carries a 697 bp BamHI to XbaI fragment generated using primers 5'AccRExt and 3'AccRExt (Table 2)	This work
$pBBR5P_N$	Gm^r, pBBR1MCS-5 derivative harbouring a P_N*::lacZ* translational fusion	23
$pBBR5P_{NI}$	Gm^r, pBBR1MCS-5 derivative harbouring a 4.2 kb BamHI to XbaI fragment that expresses the P_{NI}*::lacZ* translational fusion. The truncated P_{NI} promoter spans from position -61 to +79 with respect to the transcription start site	This work
$pIZP_{B1}$	Gm^r, pIZ1016 derivative harbouring a P_{B1}*::lacZ* translational fusion	34
pJCD-P_N	Ap^r , pJCD01 derivative harbouring a 585-bp EcoRI fragment that includes the P_N promoter	25

[a] Ap^r, ampicillin-resistant; Gm^r, gentamicin-resistant; Km^r, kanamycin-resistant; Rf^r, rifampicin-resistant; Sm^r, streptomycin-resistant.

TABLE 2
Oligonucleotides used in this study

Primers	Sequence*	Use
5'HisaccR	5'-CGGGATCCTTACCGCACCGTCCGCCGTA (BamHI)	Amplification of the 5'-end of *accR*; used to construct His-tagged *accR* and *accRD60E* genes
3'HisaccR	5'-AACTGCAGTCAGCACGTTCTGCACGAGTTCG (PstI)	Amplification of the 3'-end of *accR* gene; used to construct the *accR*, *CaccR*, and *accRD60E* genes
5'6HisCAccR	5'-CGGGATCCTTCGGCAGCTCGAGGCGGAGA (BamHI)	Amplification of the 5'-end of *CaccR*; used to construct His-tagged *CaccR*
5'AccRD60E	5'-CTCGTGCTCGAAGTGCGCATG	Internal *accR* primers used to introduce the *accRD60E* substitution
3'AccRD60E	5'-CATGCGCACTTCGAGCACGAG	
5'AccSR	5'-ACGCGTCGACTGACCTAAGGAGGTAAATAATGTCCGACT CTGCCGAATCCG (SalI)	Used to amplify and clone the *accSR* genes into plasmid pIZAccSR
3'AccSR	5'-GGACTAGTTCAGCGGCCGCCACCTCC (SpeI)	
5'AccRext	5'-CGGGATCCTAGTTAACTAGGAAGGGGGTACCATCTTCTC (BamHI)	Amplification of the *accR* gene into plasmid pBBR5AccR
3'AccRext	5'-GCTCTAGACAGGCCGGCACATCCGTCAGCG (XbaI)	
5'AccRmut(BamHI	5'-CGGGATCCGCGGAGGTCTCGCGCCAGC (BamHI)	Amplification of a 762 bp BamHI/XbaI fragment, spanning the upstream region of *accR*, for constructing the Δ*accR* allele in pKNG101Δ*accR*
3'AccRmut (XbaI)	5'-GCTCTAGACATTGTTCAGGTACGGCGGACG (XbaI)	
5'AccRmut(XbaI)	5'-GCTCTAGAGGCGGCCGCTGACGGATG (XbaI)	Amplification of the a 642 bp XbaI/SpeI fragment, spanning the downstream region of *accR*, for constructing the Δ*accR* allele in pKNG101Δ*accR*
3'AccRmut (SpeI)	5'-CCACTAGTCCATTACGCTGAGGAACCTTGCG (SpeI)	
5'pboxdQ	5'-CAACTCCAGTGCCTGTGCG	RT-PCR amplification of cDNA – a 153 bp product that reports P_D promoter activity
3'pboxdQ	5'-GAGAGGAGACAATCAGGTGAAGC	
5'RTpN1	5'-GCAACACATCAGAGGAGATAG	RT-PCR amplification of cDNA – a 141 bp product that reports P_N promoter activity
3'RTpN2	5'-GTGTAGGTACACATCGTTGC	
5´POLIIIHK	5'-CGAAACGTCGGATGCACGC	RT-PCR amplification of cDNA – a 166 bp product of *dnaE* used as internal control in RT-PCR assays
3´POLIIIHK	5'-GCGCAGGCCTAGGAAGTCGAAC	
FPAdh 5'	CGGAATTCGCACCTTCGATCCATTGCCC (EcoRI)	Amplification of a 234 bp *boxDR* intergenic fragment – P_D probe
FPAdh 3' bis	AAAAGTACTCGGTTGCTGTGATGCTGTGTC (ScaI)	
5IVTPN	CGGAATTCCGTGCATCAATGATCCGGCAAG(EcoRI)	5'-end of P_N promoter, used with 3IVTPN to amplify the 376 bp P_N probe
3IVTPN	CGGAATTCCATCGAACTATCTCCTCTGATG(EcoRI)	3'-end of P_N promoter, used to amplify the P_N, P_{N2}, and P_{N2mut} probes
5'PN3	TTTCCGCTCGCGTTCGCTCTC	Amplification of the 93 bp P_{N3} probe
3'PN3	AATCTTTCTTGCCGCAACGC	
5'PN2	AATGCAATCAAGTGCATGCAAACG	Used with 3IVTPN to amplify the 162 bp P_{N2} probe
5'PN mut3	AAACCCCTGATCAAGTGCATGCA	Used with 3IVTPN to amplify the 165 bp P_{N2mut} probe
5'ScaI P_{B1}	AAAAGTACTGGTATTACGGTAAGTGCTCCA (ScaI)	Amplification of the 251 bp P_{B1} probe
3'EcoRI P_{B1}	CCGGAATTCCCTGCGCGCGGCACTATG (EcoRI)	

* Introduced restriction sites are underlined with the corresponding enzyme given in brackets.

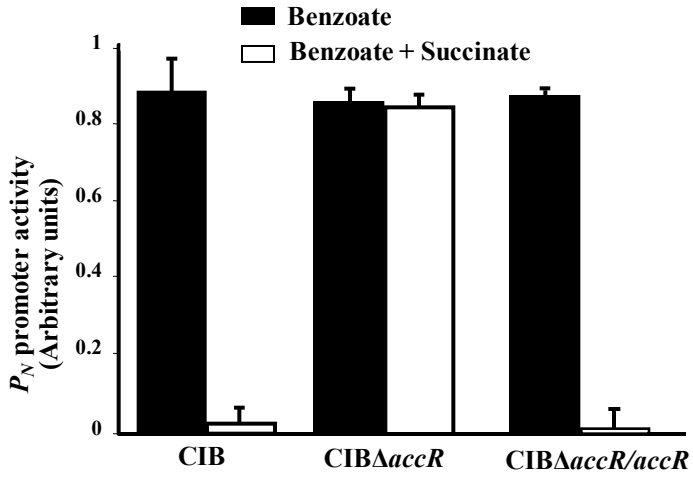
Benzoate
Benzoate + Succinate
P_N promoter activity (Arbitrary units)
1
0.8
0.6
0.4
0.2
0
CIB
CIBΔ*accR*
CIBΔ*accR/accR*

Fig. 1

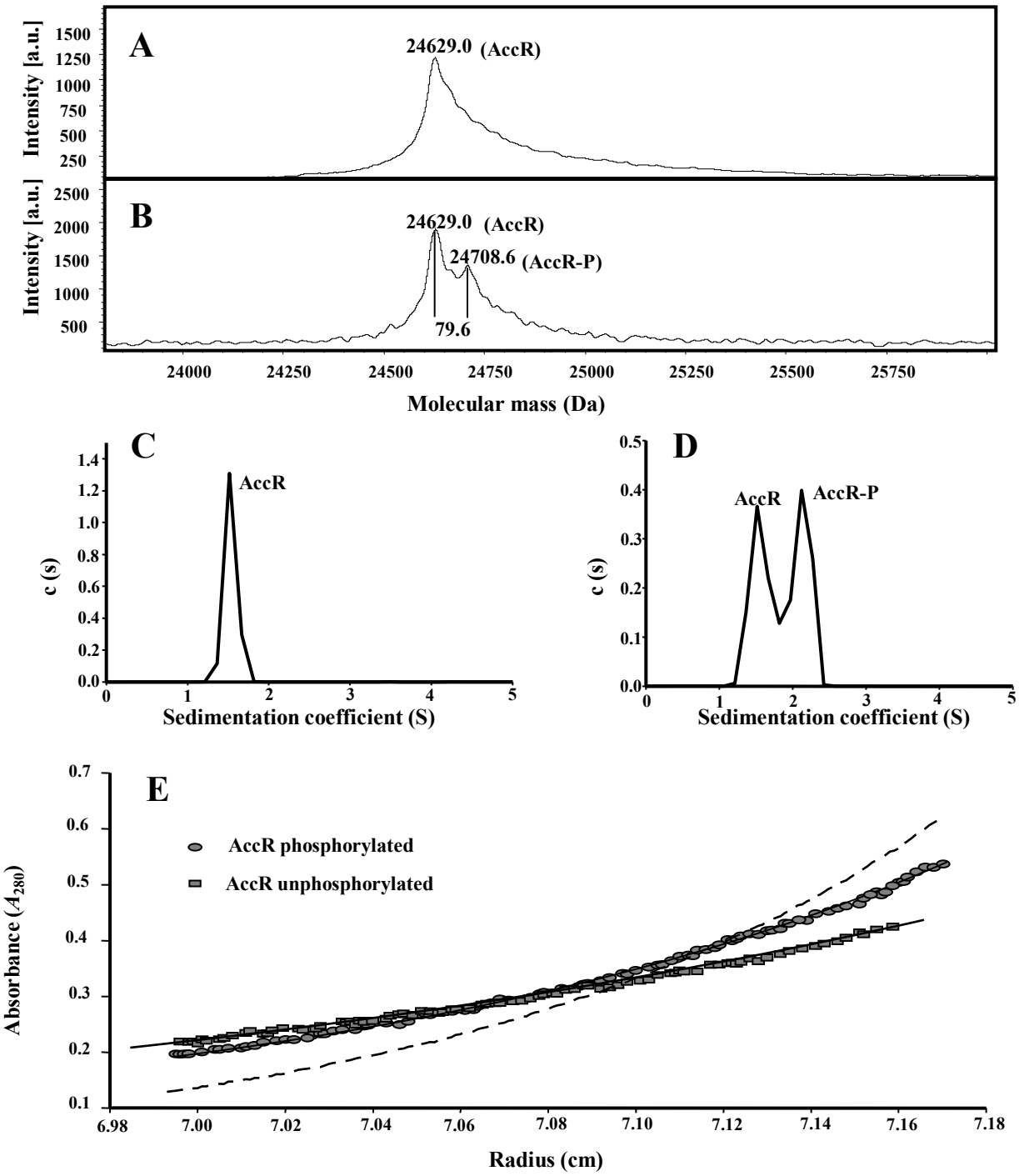
A
24629.0 (AccR)
Intensity [a.u.]
1500
1250
1000
750
500
250
B
24629.0 (AccR)
24708.6 (AccR-P)
79.6
Intensity [a.u.]
2500
2000
1500
1000
500
24000
24250
24500
24750
25000
25250
25500
25750
Molecular mass (Da)
C
AccR
c (s)
1.4
1.2
1.0
0.8
0.6
0.4
0.2
0.0
0
1
2
3
4
5
Sedimentation coefficient (S)
D
AccR
AccR-P
c (s)
0.5
0.4
0.3
0.2
0.1
0.0
0
1
2
3
4
5
Sedimentation coefficient (S)
E
AccR phosphorylated
AccR unphosphorylated
Absorbance (A_{280})
0.7
0.6
0.5
0.4
0.3
0.2
0.1
6.98
7.00
7.02
7.04
7.06
7.08
7.10
7.12
7.14
7.16
7.18
Radius (cm)

Fig. 2

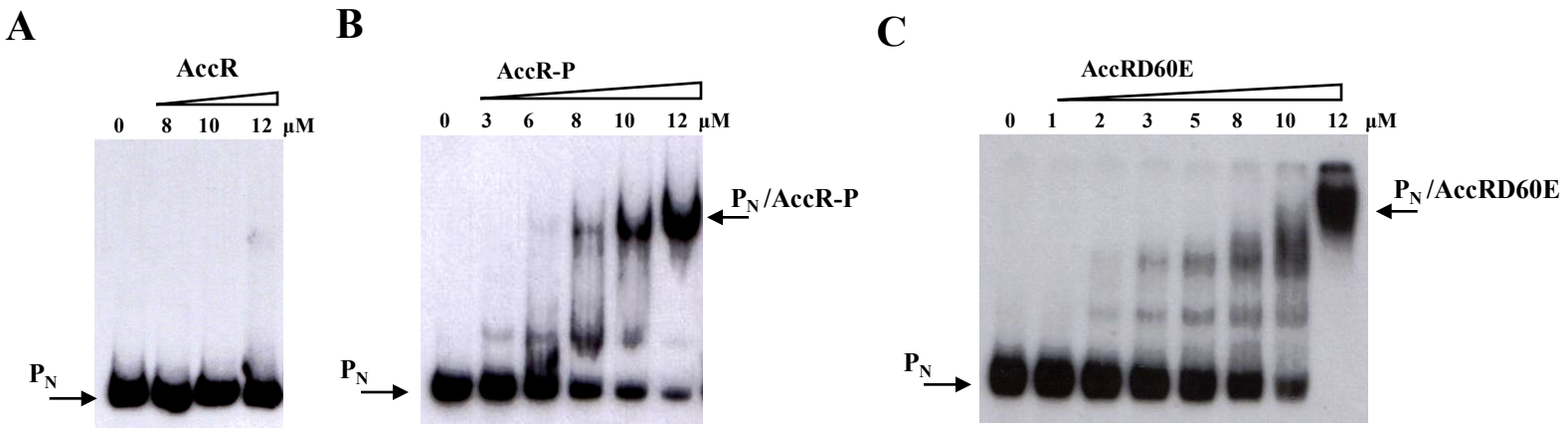
A
AccR
0 8 10 12 μM
P_N
B
AccR-P
0 3 6 8 10 12 μM
P_N
P_N/AccR-P
C
AccRD60E
0 1 2 3 5 8 10 12 μM
P_N
P_N/AccRD60E

Fig. 3

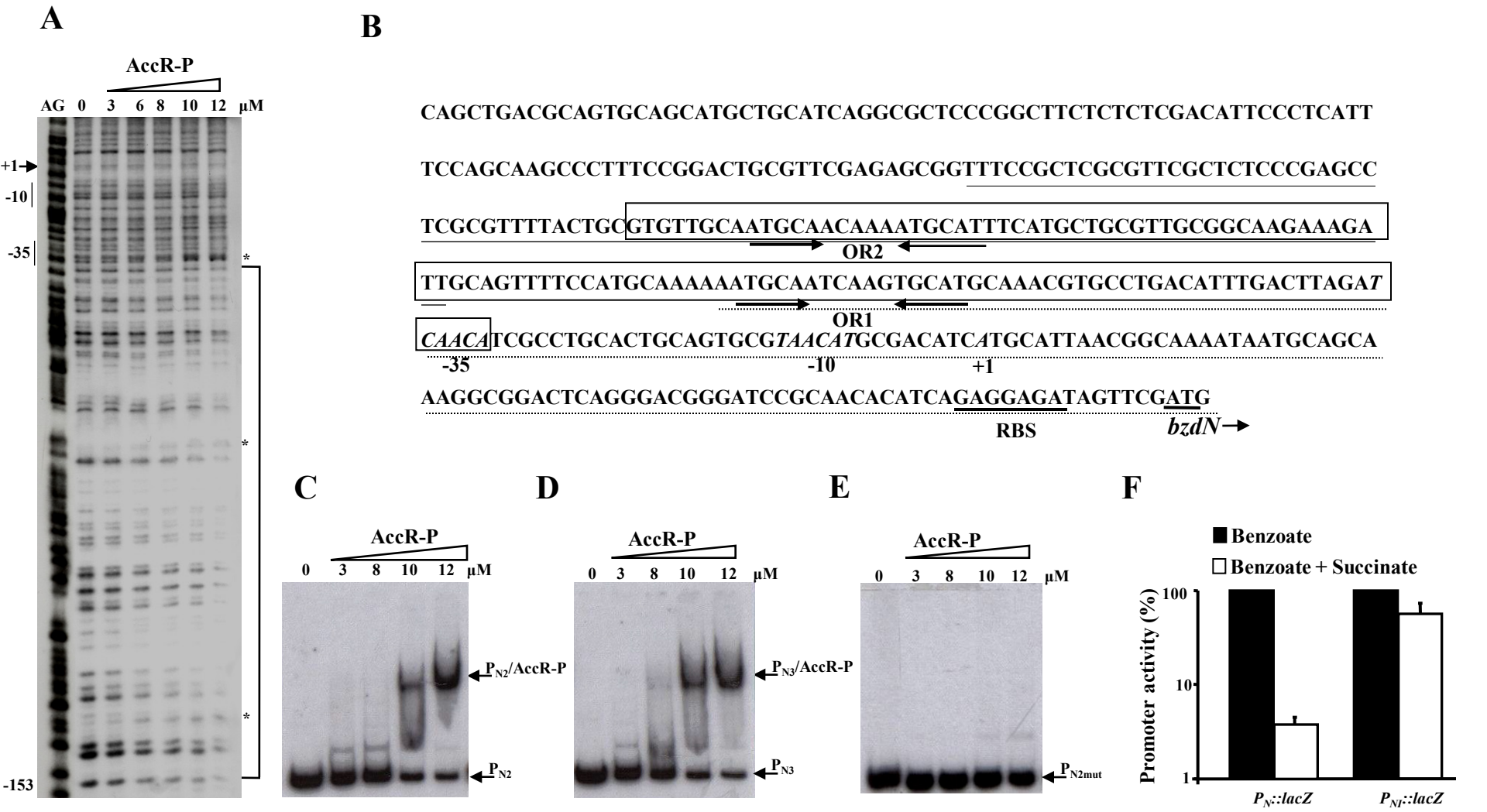
A
AccR-P
AG 0 3 6 8 10 12 μM
+1
-10
-35
-153
B
CAGCTGACGCAGTGCAGCATGCTGCATCAGGCGCTCCCGGCTTCTCTCTCGACATTCCCTCATT
TCCAGCAAGCCCTTTCCGGACTGCGTTCGAGAGCGGTTTCCGCTCGCGTTCGCTCTCCCGAGCC
TCGCGTTTTACTGCGTGTTGCAATGCAACAAAATGCATTTCATGCTGCGTTGCGGCAAGAAAGA
OR2
TTGCAGTTTTCCATGCAAAAAATGCAATCAAGTGCATGCAAACGTGCCTGACATTTGACTTAGAT
OR1
CAACATCGCCTGCACTGCAGTGCGTAACATGCGACATCATGCATTAACGGCAAAATAATGCAGCA
-35
-10
+1
AAGGCGGACTCAGGGACGGGATCCGCAACACATCAGAGGAGATAGTTCGATG
RBS
bzdN
C
AccR-P
0 3 8 10 12 μM
PN2/AccR-P
PN2
D
AccR-P
0 3 8 10 12 μM
PN3/AccR-P
PN3
E
AccR-P
0 3 8 10 12 μM
PN2mut
F
Benzoate
Benzoate + Succinate
Promoter activity (%)
100
10
1
PN::lacZ
PN1::lacZ

Fig. 4

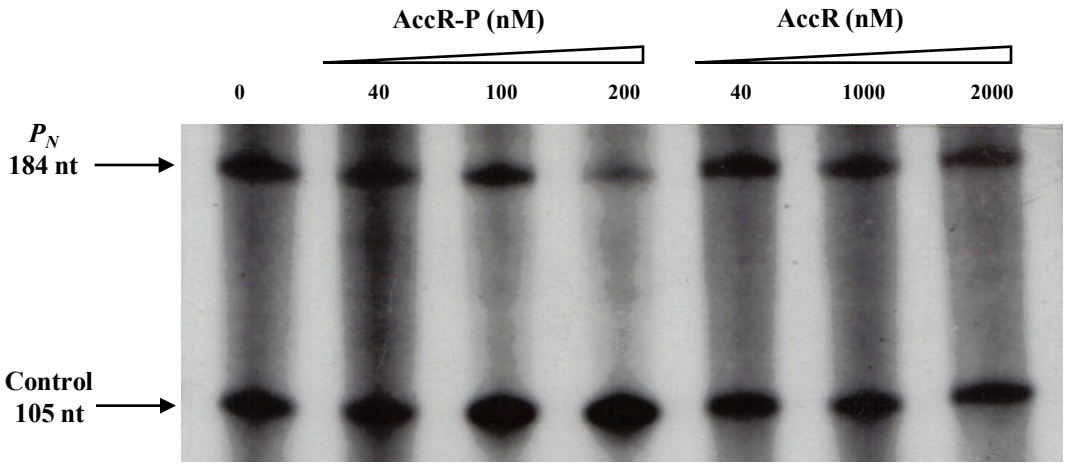
AccR-P (nM)
AccR (nM)
0
40
100
200
40
1000
2000
P_N
184 nt
Control
105 nt

Fig. 5

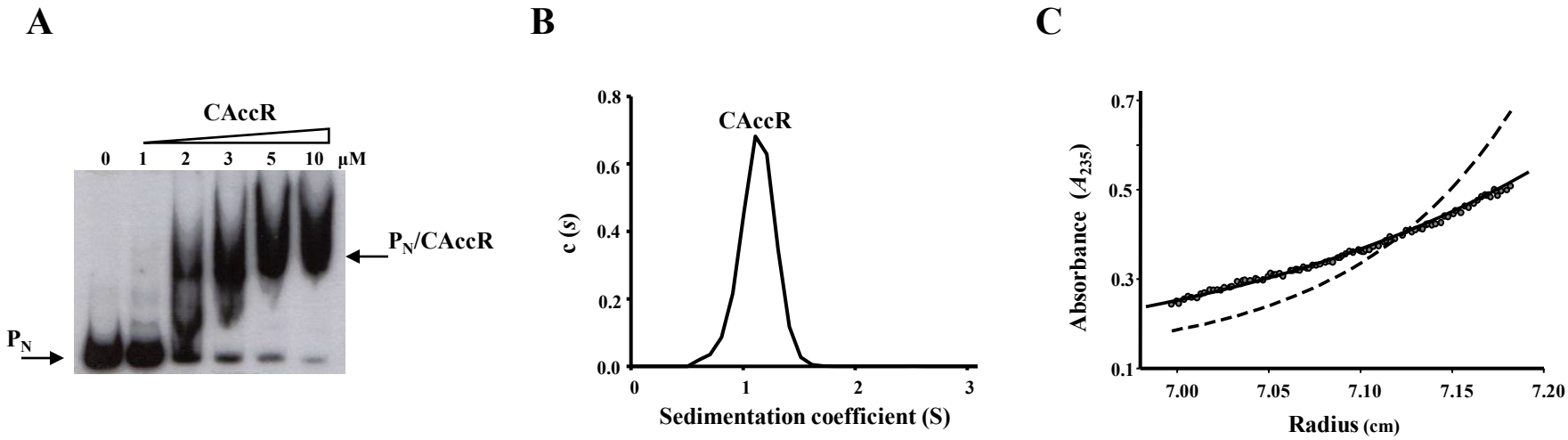
A
CAccR
0 1 2 3 5 10 μM
P_N/CAccR
P_N
B
CAccR
c (s)
0.8
0.6
0.4
0.2
0.0
0 1 2 3
Sedimentation coefficient (S)
C
Absorbance (A_{235})
0.7
0.5
0.3
0.1
7.00 7.05 7.10 7.15 7.20
Radius (cm)

Fig. 6

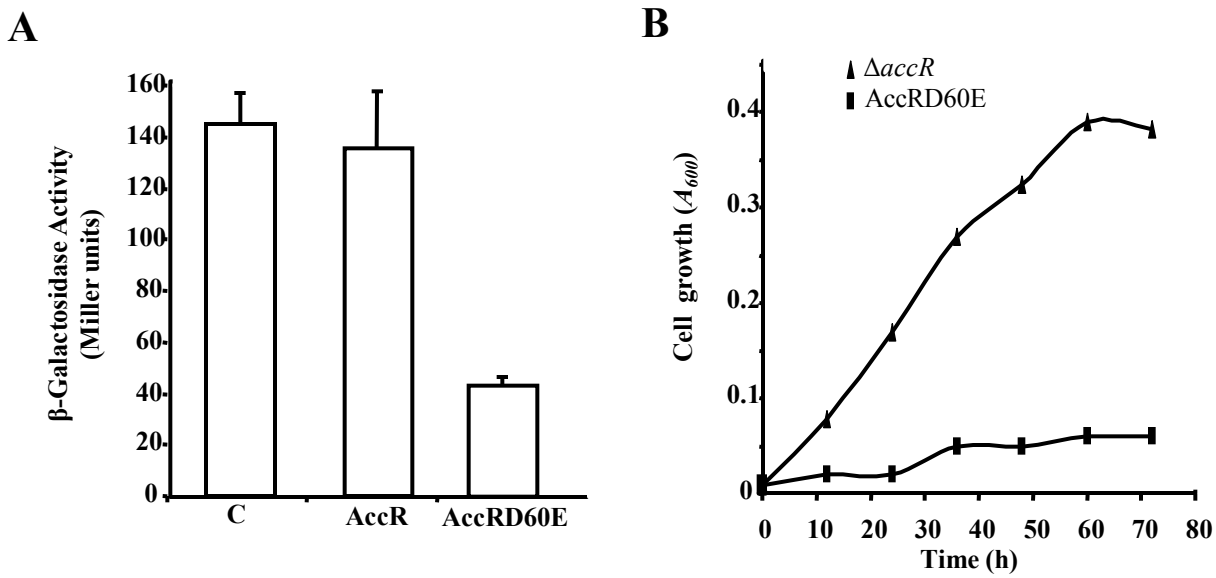
A
β-Galactosidase Activity (Miller units)
160
140
120
100
80
60
40
20
0
C
AccR
AccRD60E
B
ΔaccR
AccRD60E
Cell growth (A_{600})
0.4
0.3
0.2
0.1
0
0
10
20
30
40
50
60
70
80
Time (h)

Fig. 7

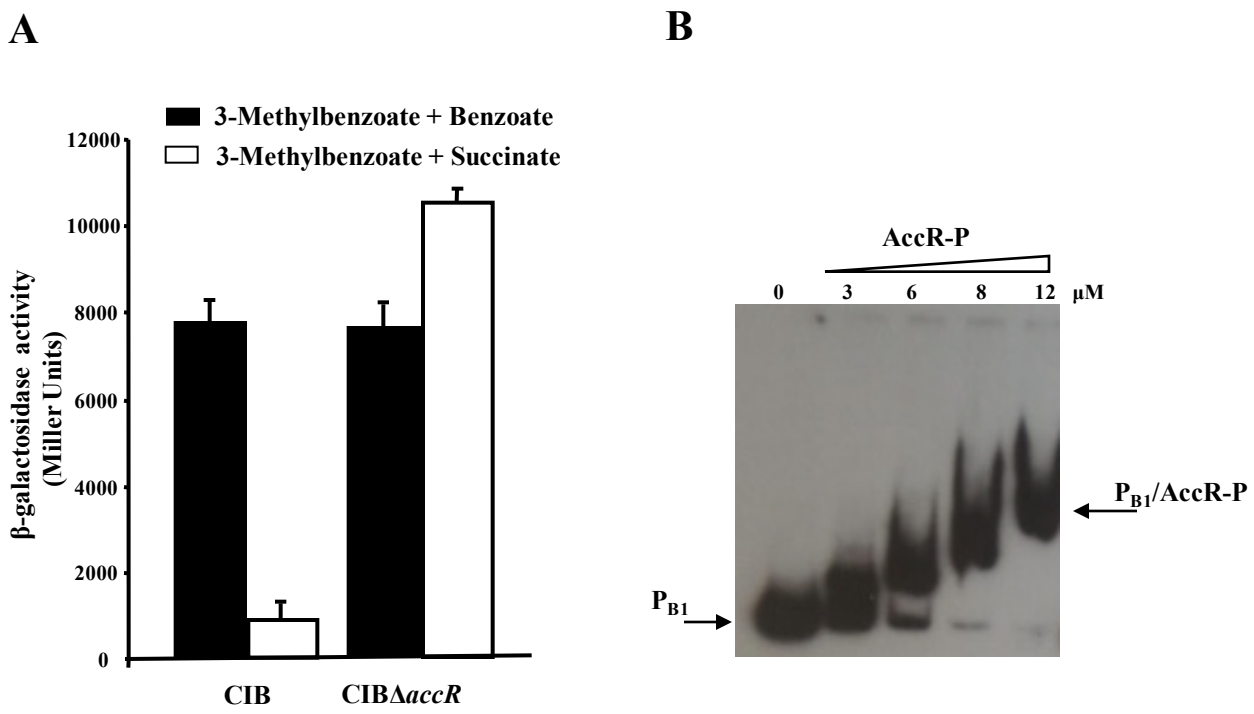
A
3-Methylbenzoate + Benzoate
3-Methylbenzoate + Succinate
β-galactosidase activity (Miller Units)
12000
10000
8000
6000
4000
2000
0
CIB
CIBΔaccR
B
AccR-P
0
3
6
8
12
μM
P_B1/AccR-P
P_B1

Fig. 8

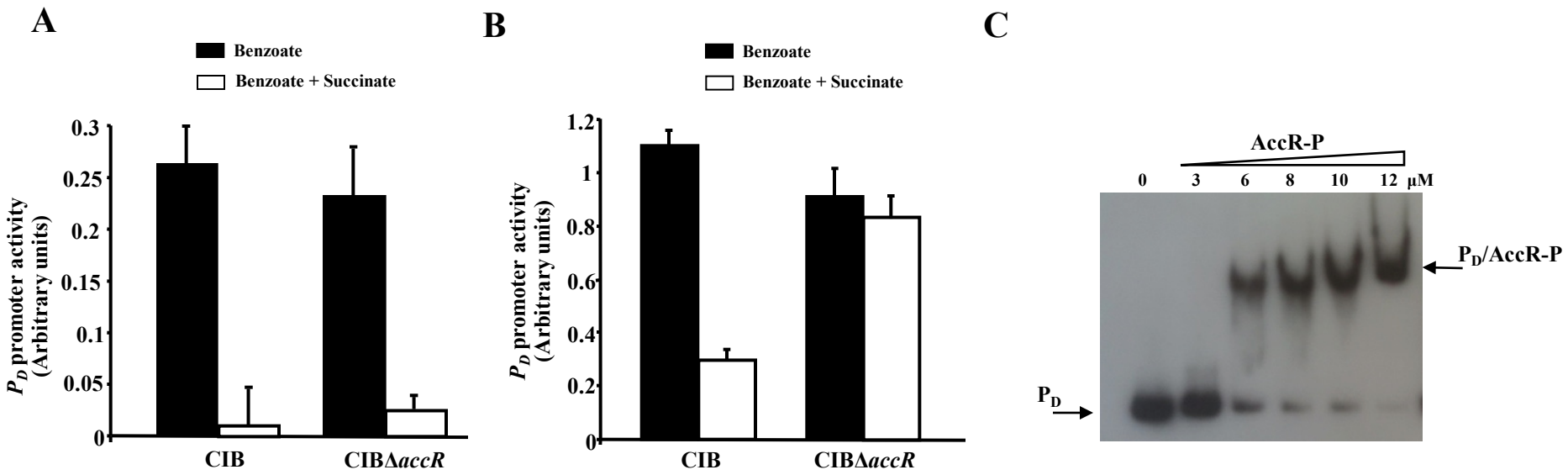

D

P_N(OR2)	TTGCA **ATGCA** ACAAAA **TGCAT** TTCATGC
P_N(OR1)	AAAAA **ATGCA** ATCAAG **TGCAT** GCAAACG
P_D	CAAAA C**TGCA** TCTT **TACAT** GGCTTGC
P_{B1}	TCGCC **ATGC**G CCG **TCCAT** GCTCTCA
Consensus	ATGCA TGCAT

Fig. 9